ChemComm

A new reductant in gold cluster chemistry gives a superatomic gold gallium cluster.

Journal:	*ChemComm*
Manuscript ID	CC-COM-10-2020-007006.R2
Article Type:	Communication

SCHOLARONE™
Manuscripts

Please do not adjust margins

COMMUNICATION

A new reductant in gold cluster chemistry gives a superatomic gold gallium cluster

Received 00th January 20xx,
Accepted 00th January 20xx

DOI: 10.1039/x0xx00000x

Florian Fetzer,[a] Claudio Schrenk,[a] Nia Pollard,[b,c] Adebola Adeagbo,[b] Andre Z. Clayborne,*[b,c] Andreas Schnepf*[a]

The low valent gallium(I) compound GaCp is primarily used in gold cluster chemistry to synthesize the superatomic cluster $[(PPh_3)_8Au_9GaCl_2]^{2+}$, complementing the borane-dominated set of reducing agents in gold chemistry, opening a whole new field for further research. Using density functional theory calculations, the cluster can be described by the jellium model as an 8-electron superatom cluster.

Metal nanoparticles are a thoroughly studied class of compounds in inorganic chemistry with various possible and partly already implemented applications.[1] These range from biomedical science[2] to electronic applications[3] all enhancing the research effort invested into nanoparticles.[4] For example, the desire to design electronic devices demands structurally well-characterized building blocks while decreasing in size.[5] Although metal nanoparticles show promising results as building blocks for thin films[6] they often lack detailed information about their exact structure and composition. At this point, atomically precise metalloid clusters of the general formula M_nX_m (M = metal, X = protecting substituent; n > m) rise as excellent model systems.[7] These compounds are often well characterized by theoreticians and experimentalists which continues to drive a growing interest in nanocluster chemistry in recent decades.[8] Investigations of atomically precise metalloid gold clusters are continually pursued heavily by chemists in part due to their size-dependent electronic properties, ligand-dependent tunable conductivity, and well-documented synthesis routes, which is prudent for both optoelectronic and biomedical applications.[9]

Since the first structural characterization of a metalloid gold cluster $Au_{11}(PPh_3)_7Cl_6$ by Malatesta *et al*. in 1969,[10] a vast amount of those clusters have been reported using varying synthesis routes. Though not identical, the majority of those routes use boranes or boranates as reducing agents, including the landmark example of the first structurally characterized multi-shell metalloid gold cluster Au_{102}(*p*-MBA)$_{44}$ (*p*-MBA = *p*-mercaptobenzoic acid).[11]

The variety of reductants successfully used for gold cluster chemistry is very meager as it is almost completely limited to boron-containing reagents with only a few exceptions of different reductants known to date.[12] As the choice of the reductant is an important parameter to determine the resulting cluster species, expanding the catalogue of viable reductants is crucial to widen the spectrum of metalloid gold clusters. The possibility of using low-valent group 13 compounds as reducing agents was already shown by Schmidbaur via the synthesis of $(dppe)_2Au_3In_3Cl_6$ (dppe = 1,2-bis(diphenylphosphino)ethane).[13]

A series of multiply doped gold clusters could successfully be synthesized via a transmetallation reaction using low-valent Al(I) and Ga(I) compounds.[12] The introduced dopants alter the electronic state of the resulting clusters. The formation of gold clusters by the utilization of a gallium (I) precursor as reductant without transition-metal doping was primarily described by Sharp *et al.*in 2004.[14] Thereby, in addition to their functionality as a reducing agent gallium(I) compounds can be used to incorporate gallium atoms into the resulting cluster due to the tendency to insert into the gold-halide bonds.[15] These combined properties of inserting gallium into the gold halide bond while simultaneously reducing the gold atom qualifies subvalent gallium precursors as possible reductants to form intermetalloid gold clusters. Thereby, the chosen ligand coordinated to the gallium precursor can have an immense impact onto the reductive behavior of the compound. Examples are Ga-DDP (DDP =2-((2,6-diisopropylphenyl)amino-4-((2,6-diisopropylphenyl)imino)-2-pentene) whose reductive properties are yet only proven for tin with the synthesis of the metalloid cluster $[Sn_{17}(GaCl(DDP))_4]$,[16] and GaCp* (Cp* =

[a] *Institute of Inorganic Chemistry, Universität Tübingen, Auf der Morgenstelle 18, D-72076 Tübingen, Germany.*
[b] *Department of Chemistry, Howard University, 525 College Street NW, Washington, District of Columbia, United States of America.*
[c] *Department of Chemistry and Biochemistry, George Mason University, 4400 University Drive MSN 3E2, Fairfax, Virginia, United States of America*
*Prof. Dr. A. Schnepf, Tel.: Int. Code +49 (7071) 29 – 76635; Fax: Int. Code +49 (7071) 28 – 2436; Email: andreas.schnepf@uni-tuebingen.de; Prof. A. Clayborne, Tel:+1 (703) 993 - 1070 ; Email: aclaybo@gmu.edu

† Electronic Supplementary Information (ESI) available: [details of any supplementary information available should be included here]. See DOI: 10.1039/x0xx00000x

Please do not adjust margins

pentamethylcyclopentadienyl) which was already used as a reductant in gold chemistry.[14] Unlike many of the known gallium(I) species which afford comparatively complex

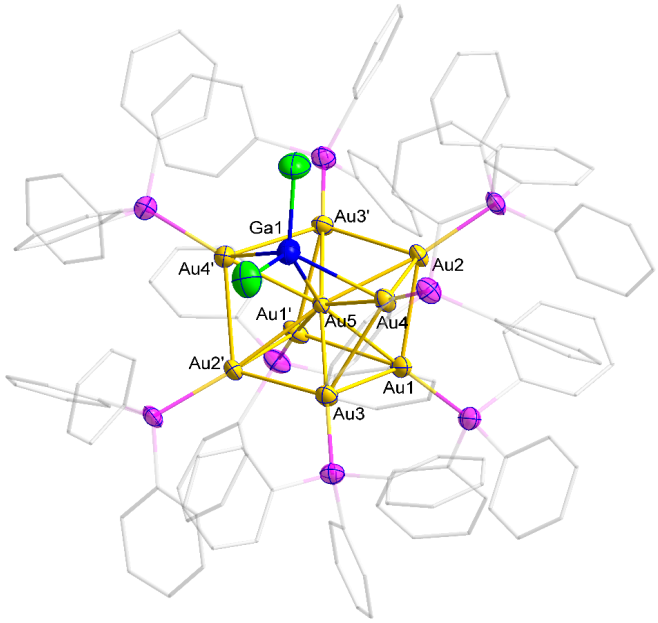

Figure 1 Molecular structure of $[(PPh_3)_8Au_9GaCl_2]^{2+}$ in the solid state. All atoms except for carbon are displayed as thermal ellipsoids with 50% probability. Hydrogen atoms are omitted for clarity. Au: gold, Ga: blue, P: violet, Cl: green. Selected bond lengths [pm] and angles [°]: Au1-Au1‘ 320.1, Au1-Au2 289.4, Au1-Au3 287.6, Au1-Au5 263.4, Au2-Au3 283.6, Au2-Au4 289.4, Au2-Au5 272.7, Au3-Au4 293.9, Au3-Au5 267.8, Au4-Au5 267, Au4-Ga 268.6, Au5-Ga 247.1, Ga-Cl 220.7; Au2-Au5-Au2' 163.961(20), Au1-Au5-Au4‘ 154.475(17), Au4-Ga-Au4' 124.401(19), Au4'-Au3'-Au2 110.830(27), Au3'-Au2-Au4 107.429(26), Au1'-Au1-Au3 87.123(22), Au1-Au3-Au2' 93.061(25), Au3-Au2'-Au1' 94.121(24), Au2'-Au1'-Au1 85.558(22), Au4-Ga-Auf4‘ 124.401(19), Cl-Ga-Cl 104.055(139), Symmetry operations: 1-x, y, 3/2-z.

syntheses[18] gallium cyclopentadienyl (GaCp) can be prepared easily in a one-step synthesis. It is thus accessible by a reaction of GaI and NaCp as previously published by our group.[19]

The reaction of in-situ generated GaCp with PPh_3AuCl in toluene at room temperature yields a dark red solid. The title compound $[(PPh_3)_8Au_9GaCl_2]^{2+}$ **1** with $[GaCl_4]^-$ and $[GaCpCl_3]^-$ as counter anions can be crystallized after dissolving the red solid in a thf/diethyl ether mixture (for further information see SI). The crystals were suitable for single crystal x-ray diffraction and the obtained structure of the title compound **1** is displayed in figure 1.[20] **1** crystallizes with the counter ions in the monoclinic space group *C*2/c, whereby half a molecule is present within the asymmetric unit. **1** has a kernel built of nine gold atoms and one $GaCl_2$ unit. A triphenylphosphine group is bound to each peripheral gold atom. The kernel structure formed by the nine gold atoms resembles the $[Au_9(P(p\text{-}C_6H_4OMe)_3)_8]^{3+}$ cluster, published by Mingos *et al*. in 1982.[21] In compound **1**, the incorporated $GaCl_2$ unit is shifted out of plane and leads to a distortion of the kernel compared to the one published by Mingos *et al.* The whole core is therefore best described as a truncated Au-centered centaur polyhedron (Au_9Ga) with one corner missing and another one occupied by the $GaCl_2$-unit. This motif of a centered centaur polyhedron is already well described in gold cluster chemistry within the structures of various $Au_{11}(PPh_3)_7X_3$-cluster species (X = Cl, SCN, CN^iPr, I).[22] The model of a truncated centaur polyhedron is supported by the bond angles of 107.43° and 110.83° for Au3'-Au2-Au4 and Au4'-Au3'-Au2 respectively, which are close to the angle of 108° of an ideal pentagon. The Au-Au distances between the peripheral gold atoms (283.6 pm and 293.9 pm) are in the range known for elemental gold (288 pm). The bond lengths to the central gold atom are shorter, which is consistent with the observations of Hutchison *et al*. on an Au-centered centaur polyhedron.[23] Within **1** two Au-Ga distances are present. The Au-Ga distance to the outer gold atoms (Au4-Ga) is with 268.6 pm in the range found within an Au-Ga alloy.[24] In contrast to this the Au-Ga distance to the central gold atom is with 247.1 pm remarkably shorter.

The two counter anions are a superposition of a 60:40 ratio of $GaCpCl_3^-$ and $GaCl_4^-$ respectively, as found during crystal structure determination. These display the oxidation products of the employed reducing agent GaCp. The ratio is confirmed by NMR spectroscopy (see SI for further information).

Quantum chemical calculations shed light on the “superatom” nature of the cluster system. The quantum chemical calculations were performed using the GPAW code with the PBE functional for exchange and correlation using the structure determined by x-ray analysis of **1** and an alternative structure by reducing the ligands to methyl groups ($\mathbf{1_{Me}}$) (Figure 2). For precise details see supporting information. Table S1 in the SI shows the bond lengths of the computed ground state structures for **1** and $\mathbf{1_{Me}}$. We note that the bond lengths of the relaxed structures differ only by 2.84% when compared to the experimentally obtained structure (Table S1). In the superatom view (i.e., jellium) the molecular orbitals on the cluster core arise from the iterant valence electrons of the metal atom core. Here, the total number of electrons contributing to the molecular orbital configuration is eight or $1S^21P^6$. An analysis of the spherical Kohn-Sham orbital density indicates that the highest occupied molecular orbital in **1** and $\mathbf{1_{Me}}$ has P-symmetry. While both **1** and $\mathbf{1_{Me}}$ have a HOMO state of P-symmetry, the reduction of the ligand assists in gaining clarity

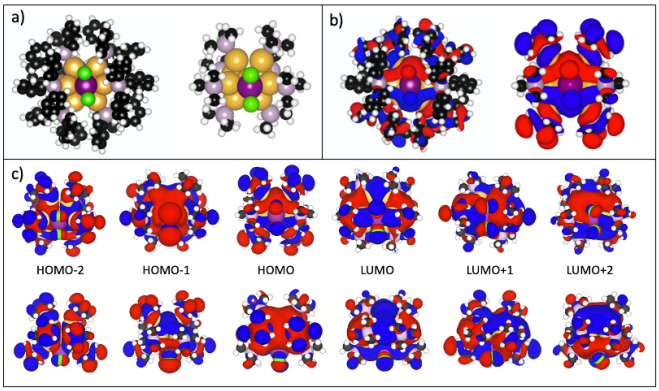

Figure 2 Visualization of computational results of **1** and $\mathbf{1_{Me}}$. (a) Space filling model of **1** (left) and $\mathbf{1_{Me}}$ (right). The black, white, pink, gold, purple, and green balls represent the C, H, P, Au, Ga, and Cl atoms respectively. (b) Kohn-Sham density of the highest occupied molecular orbitals for **1** (left) and $\mathbf{1_{Me}}$ (right). (c) Kohn-Sham density of the three highest occupied molecular orbitals (HOMO) and lowest unoccupied molecular orbitals (LUMO) of **1** (up) and $\mathbf{1_{Me}}$ (down).

This journal is © The Royal Society of Chemistry 20xx

of the electron density residing on the core. A close view of the three highest occupied and three lowest unoccupied orbitals reveal P and D symmetry respectively (Figure 2). The HOMO-LUMO gap is 1.81 eV and 1.84 eV for **1** and $\mathbf{1_{Me}}$ respectively. The orbital symmetry and large HOMO-LUMO gap are characteristics that illustrate the superatom character of the cluster.

Despite this superatom character of the cluster, a slow degradation of **1** in solution can be observed as shown by NMR experiments (see SI). Stability of **1** against oxygen or moisture was probed by contaminating a solution of **1** with air and water, respectively. The reaction was monitored by NMR spectroscopy, showing a rapid degradation of **1** within a few hours. The degradation products could not be isolated or identified yet. Further information about the cluster, its stability and decomposition could be obtained by high-resolution electro-spray-ionization mass spectrometry (HR-ESI-MS). The degradation products that could be identified are displayed in figure 4. Degradation of **1** due to oxygen or moisture contamination during the transfer into the spectrometer cannot be ruled out completely, despite no oxygen-containing compounds could be observed. The title compound $[(PPh_3)_8Au_9GaCl_2]^{2+}$ could be assigned to the peak at 2005.63661 m/z corresponding to the molar mass of 4011.65 g/mol and the double positive charge of **1**. Some degradation products could be identified which gives insight into the decomposition processes of **1** during the transfer to the gas-phase (Figure 4). The smallest fragment that could be detected by HR-ESI-MS is the literature-known $(PPh_3)_2Au^+$ **2**.[25] Further degradation products are $[Au_6(PPh_3)_6]^{2+}$ **3** and $[Au_8(PPh_3)_7]^{2+}$ **4** which could be identified by their mass of 1377.67 m/z and 1705.677 m/z, respectively. The formation of **3** can be explained

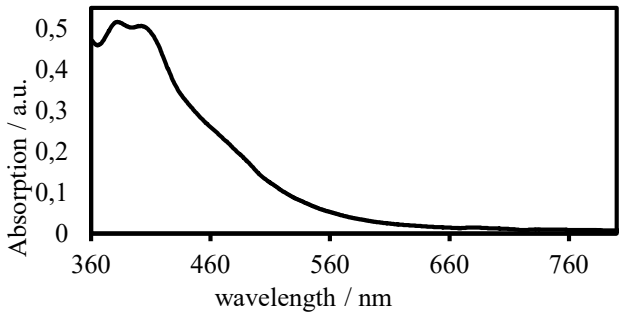

Figure 3 UV-vis spectrum of title compound $[(PPh_3)_8Au_9GaCl_2]^{2+}$ **1** in dichloromethane. The spectrum shows two clear peaks at 385 nm and 405 nm.

Table 1. Electronic transitions observed in the 1ME simulated UV-Vis spectra.

nm	eV	From	Symmetry	To	Symmetry
408	3.04	HOMO-6	hybrid	LUMO	1D
394	3.15	HOMO-2	1P	LUMO+3	1D
374	3.31	HOMO-1	1P	LUMO+4	1D

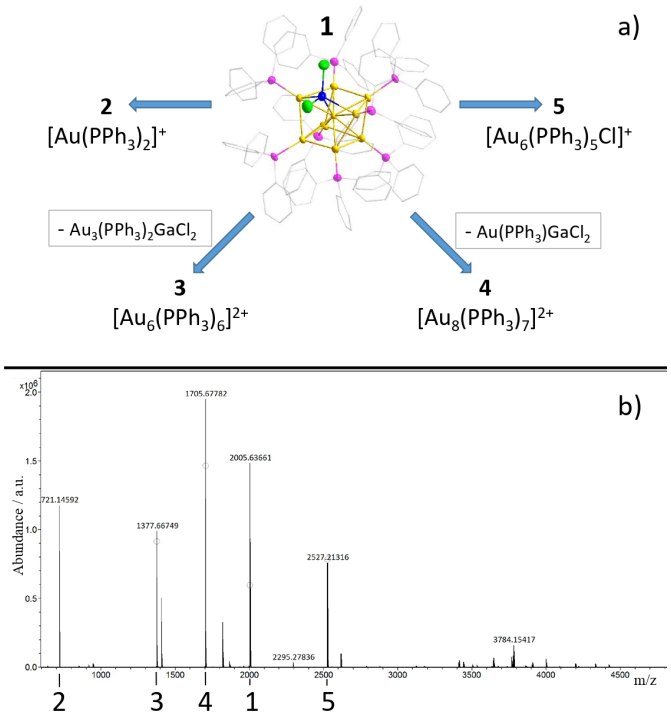

Figure 4 a) Scheme of the degradation of $[(PPh_3)_8Au_9GaCl_2]^{2+}$ during the gas phase transfer. b) Overview of the spectrum, showing the intact cluster at 2005.63661 m/z and several degradation products (for further information see SI).

by the elimination of a $(PPh_3)_2Au_3GaCl_2$-group from **1**. Beside this, compound **4** results from the elimination of the smaller group $(PPh_3)AuGaCl_2$ from the title compound **1**. The degradation products **2**,**3** and **4** are all already known as gas-phase species and were previously observed in ESI-MS measurements.[26] It is important to note, that the degradation products observed do not contain gallium atoms. This implies that the removal of the $GaCl_2^+$ group may be an early step in the degradation of **1**. The resulting $Au_9(PPh_3)_8^+$ cluster also shows quick decomposition in solution despite its eight-electron closed-shell electronic structure as described by Häkkinen, Zheng and co-workers.[27] The metastability of **1** suggests that while electronic structure is typically a good indicator of stability, there are other factors (i.e., thermodynamics) that may play a role, similar to gold-thoilates.

The optical properties of **1** have been investigated by UV-vis spectroscopy (Figure 3), showing some characteristic features. Two prominent peaks are observed at wavelengths of 385 nm and 405 nm which is in the range of previously reported absorption maxima of gold clusters.[23] We compared the experimental UV-Vis spectrum to the simulated one of $\mathbf{1_{Me}}$ (details in supporting information) to gain clear insight into the origins of the electronic transitions contributing to the prominent peaks. At 408 nm, the transition originated from a state 1.15 eV below the highest occupied molecular orbital (HOMO-6) and transitions to the lowest unoccupied state (LUMO). There are two peaks in the simulation that could correspond to the observed peak at 385 nm. The simulations

point to two peaks at 394 nm and 374 nm. Both of these originate from superatom 1P-states (Table 1).

We reported the synthesis and characterization of an atomically precise intermetalloid gold-gallium cluster $[(PPh_3)_8Au_9GaCl_2]^{2+}$ **1,** obtained by the reduction of an Au(I)-precursor by the low-valent gallium species GaCp. It is the first successful synthesis of a metalloid gold cluster using GaCp as a reducing agent, opening the door to a new cluster family. The reported reduction system also displays a viable alternative to the transmetallation reactions reported by Fischer *et al.* to generate gallium doped gold clusters.[12] **1** has been characterized by NMR, single crystal X-ray analysis and HR-ESI-MS. The mass spectrometric investigations reveal various degradation products, giving insight into the degradation process of the cluster. Quantum chemical calculations support the classification of the compound as an eight-electron superatom complex and identified origins of the prominent peaks in the UV-Vis spectra.

This cluster is the first example of an intermetalloid cluster obtained by using GaCp as a reductant. The easy accessibility and fast in-situ generation of GaCp allows this compound to be used in a manifold of reaction systems and thereby opens up a huge field for further research.

Acknowledgements

F. Fetzer thanks the PhD Network: "Novel nanoparticles: from synthesis to biological applications" at the university Tübingen for financial support. We thank Florian Pachel for his support during the DTG measurements. A. Clayborne, N. Pollard, and A. Adeagbo thank the National Science Foundation (USA) for financial support (NSF 1831559). This work used the Extreme Science and Engineering Discovery Environment (XSEDE), which is supported by National Science Foundation grant number ACI-1548562. Specifically, it used the Bridges system, which is supported by NSF award number ACI-1445606, at the Pittsburgh Supercomputing Center (PSC).

Conflicts of interest

There are no conflicts to declare.

Notes and references

1 H. Goesmann and C. Feldmann, *Angew. Chem*. 2010, **122**, 1402.
2 J. G. Fujimoto and D. Farkas in *Biomedical Optical Imaging*, Oxford University Press, Oxford, 2009
3 (*a*) A. L. Briseno, S. C. B. Mannsfeld, M. M. Ling, S. Liu, R. J. Tseng, C. Reese, M. E. Roberts, Y. Yang, F. Wudl and Z. Bao, *Nature*, 2006, **444**, 913; (b) T. Kraus, L. Malaquin, H. Schmid, W. Riess, N. D. Spencer and H. Wolf, *Nat. Nanotechnol*. 2007, **2**, 570; (*c*) D. L. Klein, R. Roth, A. K. L. Lim, A. P. Alivisatos and P. L. McEuen, *Nature*, 1997, **389**, 699; (*d*) P. P. Edwards, S. R. Johnson, M. O. Jones and A. Porch in *Molecular Nanowires and other Quantum Objects*, Kluwer Academic Publishers, London, 2004, p. 329; (*e*) G. Hodes, *Adv. Mater*. 2007, **19**, 639.
4 R. F. Service, *Science*, 1996**, 271**, 920.
5 (*a*) C. R. Kagan, E. Lifshitz, E. H. Sargent and D. V. Talapin, *Science*, 2016, **353**, aac5523; (*b*) G. Schmid, *Adv. Eng. Mater*., 2001, **3**, 737.
6 A. Zabet-Khosousi and A. Dhirani, *Chem. Rev*., 2008, **108**, 4072.
7 A. Schnepf in *Clusters – Contemporary Insight in Structure and Bonding* (Ed.: J. S. Dehnen), Structure and Bonding Vol. 174, 2017, pp. 135-200.
8 (*a*) K. P. Hall and D. M. P. Mingos, *Prog. Inorg. Chem*., 1984, **32**, 237; (*b*) G. Schmid, *Chem. Rev*. 1992, **92**, 1709; (*c*) M. Daniel and D. Astruc, *Chem. Rev*. 2004, **104**, 293.
9 (*a*) V. Torma, G. Schmid and U. Simon, *ChemPhysChem*, 2001, **2**, 321; (*b*) M. Galchenko, A. Black, L. Heymann and C. Klinke, *Adv. Mater*. 2019, **31**, 1900684.
10 M. McPartlin, R.Mason and L. Malatesta, *J. Chem. Soc D.: Chem. Commun.* 1969, **7**, 334.
11 (*a*) C. E. Briant, K. P. Hall, A. C. Wheeler and D. M. P. Mingos, *J. Am. Chem. Soc., Chem. Comm*., 1984, 248; (*b*) P. D. Jadzinsky, G. Calero, C. J. Ackerson, D. A. Bushnell and R. D. Kornberg, *Science*, 2007, **318**, 430; (*c*) N. A. Sakthivel, S. Theivendran, V. Ganeshraj, A. G. Oliver and A. Dass, *J. Am. Chem. Soc*. 2017, **139.43**, 15450; d) S. Kenzler, C. Schrenk and A. Schnepf, *Angew. Chem. Int. Ed*., 2017, **56.1**, 393.
12 A. Puls, P. Jerabek, W. Kurashige, M. Förster, M. Molon, T. Bollermann, M. Winter, C. Gemel, Y. Negishi, G. Frenking and R. A. Fischer, *Angew. Chem. Int. Ed*. 2014, **53**, 4327.
13 F.P.Gabbai, A.Schier, J.Riede and H.Schmidbaur, *Inorg.Chem*. 1995, **34**, 3855.
14 U. Anandhi and P. R. Sharp, *Angew. Chem. Int. Ed*. 2004, **43**, 6128.
15 A. Kempter, C. Gemel and R. A. Fischer, *Inorg. chem*. 2005, **44.2**, 163.
16 G. Prabusankar, A. Kempter, C. Gemel, M. Schröter and R. A. Fischer, *Angew. Chem. Int. Ed*. 2008, **47**, 7234.
17 R. J. Baker and C. Jones, *Dalton Trans*., 2005, **8**, 1341.
18 (*a*) D. Loos, H. Schnöckel, *J. organomet. chem*. 1993, **463**, 37; (*b*) N. J. Hardman, B. E. Eichler, P. P. Power, Chem. Comm. 2000, 1991-1992.
19 C. Schenk, R. Köppe, H. Schnöckel and A. Schnepf*, Eur. J. Inorg. Chem*. 2011, **25**, 3681.
20 Crystal data of 1: M=4471.45 g/mol, monoclinic, C2/c, a=31.0956(13) Å, b=15.1623(6) Å, c=33.4620(14) Å, β=97.4410(10), V=15643.8(11) Å3, μ=9.188 mm-1, ρ=1.899 g/cm³, 15977 independent reflections, R(int)=0.0891, R1(I>2σ)=0.0523, wR2 (all data)=0.1425, T=150 K. CCDC Number: 2032544. For further details see the crystallographic section in the Supporting Information.
21 K. P. Hall, B. R. Theobald, D. I. Gilmour, D. M. P. Mingos and A. J. Welch, *J. Chem. Soc., Chem. Commun*. 1982, **10**, 528.
22 (*a*) M. McPartlin, R. Mason and L. Malatesta, *Chem. Comm*., 1969, 7, 334; (*b*) W. Bos, R. V. Kanters, C. J. Van Halen, W. P. Bosman, H. Behm, J. M. M. Smits, P. T. Beurskens, J.J Bour and L. H. Pignolet, *J. organomet. chem*., 1986**, 307.3**, 385; (*c*) V.G. Albano, P. L. Bellon, M. Manassero and M. Sansoni, *Chem. Comm*. 1970, **18**, 1210.
23 L. C. McKenzie, T. O. Zeikova and J. E. Hutchison, *J. Am. Chem. Soc*. 2014, **136.38**, 13426.
24 H. Pfisterer and K. Schubert, *Naturwissenschaften*, 1950, **37.5**, 112.
25 A. Zhdanko, M. Ströbele and M. E. Maier. *Chem. Eur. J*. 2012, **18.46**, 14732.
26 M. A. Hewitt, H. Hernández and G. E. Johnson, *J. Phys. Chem. C*, 2020, **124**, 3396.
27 H. Shen, E. Selenius, P. Ruan, X. Li, P. Yuan, O. Lopez-Estrada, S. Malola, S. Lin, B. Teo, H. Häkkinen and N. Zheng, *Chem. Eur. J*. 2020, **26**, 8465

 This journal is © The Royal Society of Chemistry 20xx